Electronic Supplementary Material (ESI) for Journal of Materials Chemistry C.

Electronic Supplementary Information

Highly responsive and selective ppb-level NO_2 gas sensor based on mesoporous Pd-functionalized CuO/rGO at room temperature

Haineng Bai[1], Hui Guo[1], Cheng Feng[2], Jin Wang[3], Bin Liu[1], Zili Xie[1], Fuqiang Guo[2*], Dunjun Chen[1*], Rong Zhang[1], Youdou Zheng[1]

[1] *Key Laboratory of Advanced Photonic and Electronic Materials, School of Electronic Science and Engineering, Nanjing University, Nanjing 210023, China. E-mail: djchen@nju.edu.cn*

[2] *Department of Physics, Changji University, Xinjiang, Changji 831100, China. E-mail: cjxyedu@163.com*

[3] *College of Electronic and Optical Engineering & College of Microelectronics, Nanjing University of Posts and Telecommunications, Nanjing 210023, China*

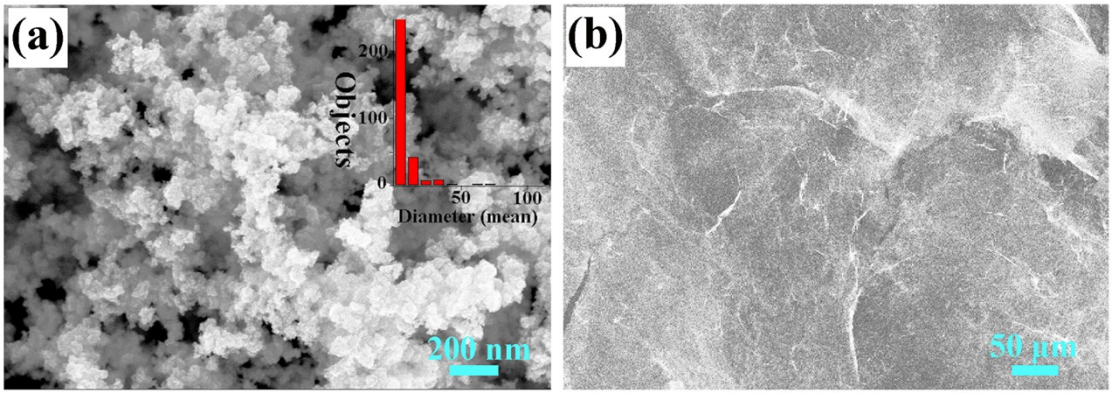

Fig. S1. SEM images of (a) Pd NPs and (b) rGO NSs.

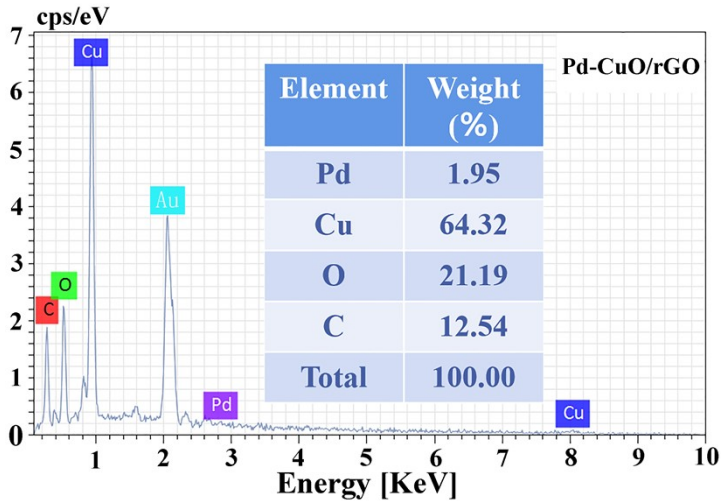

Fig. S2. EDX images of Pd-CuO/rGO.

Herein, the gold-spray treatment was applied on the surface of material due to the test requirement, so Au element was found in EDX, but the EDX result of the material was obtained by removing the proportion of Au element.

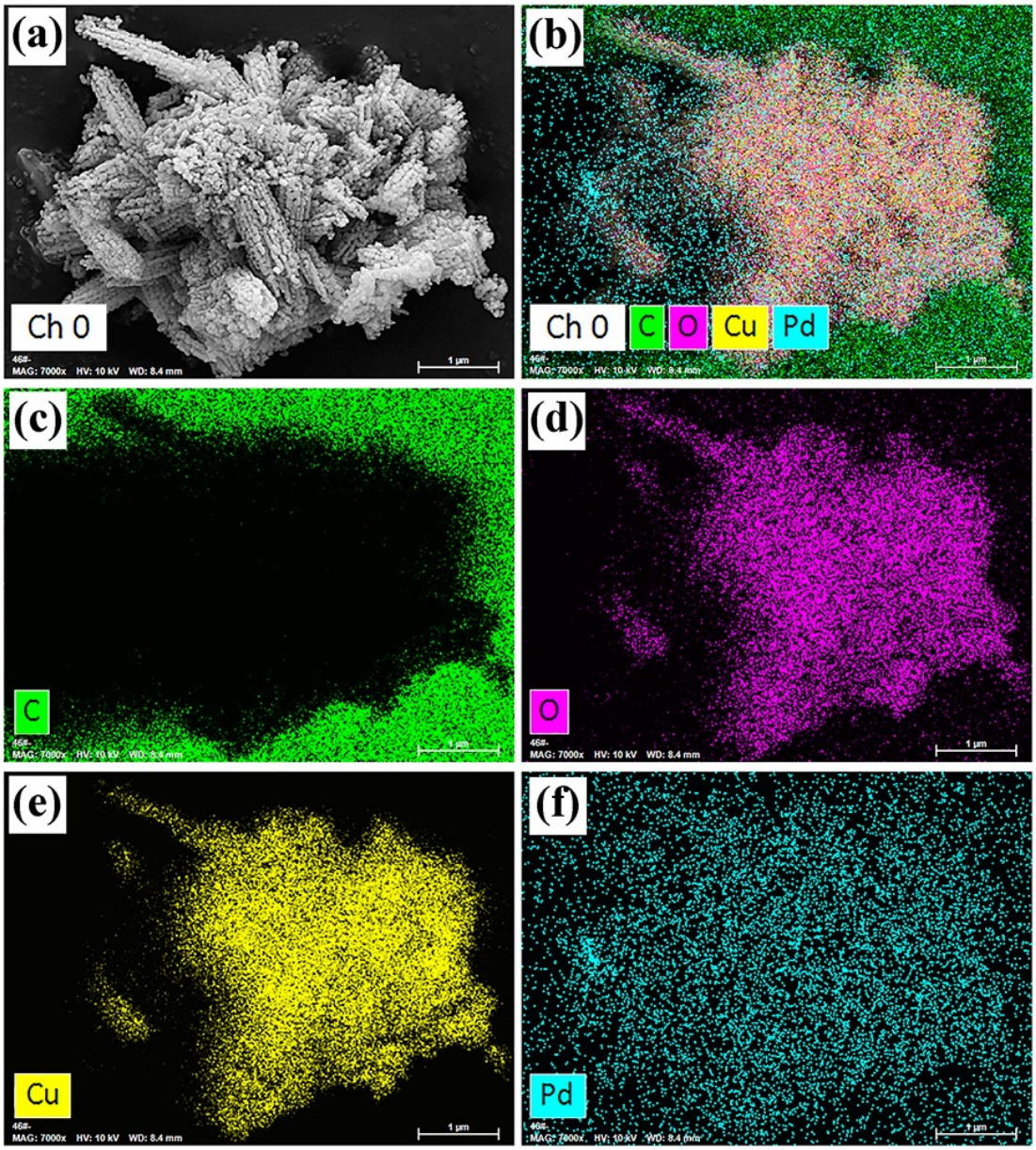

Fig. S3. SEM element mappings of Pd-CuO/rGO and corresponding elemental mapping images.

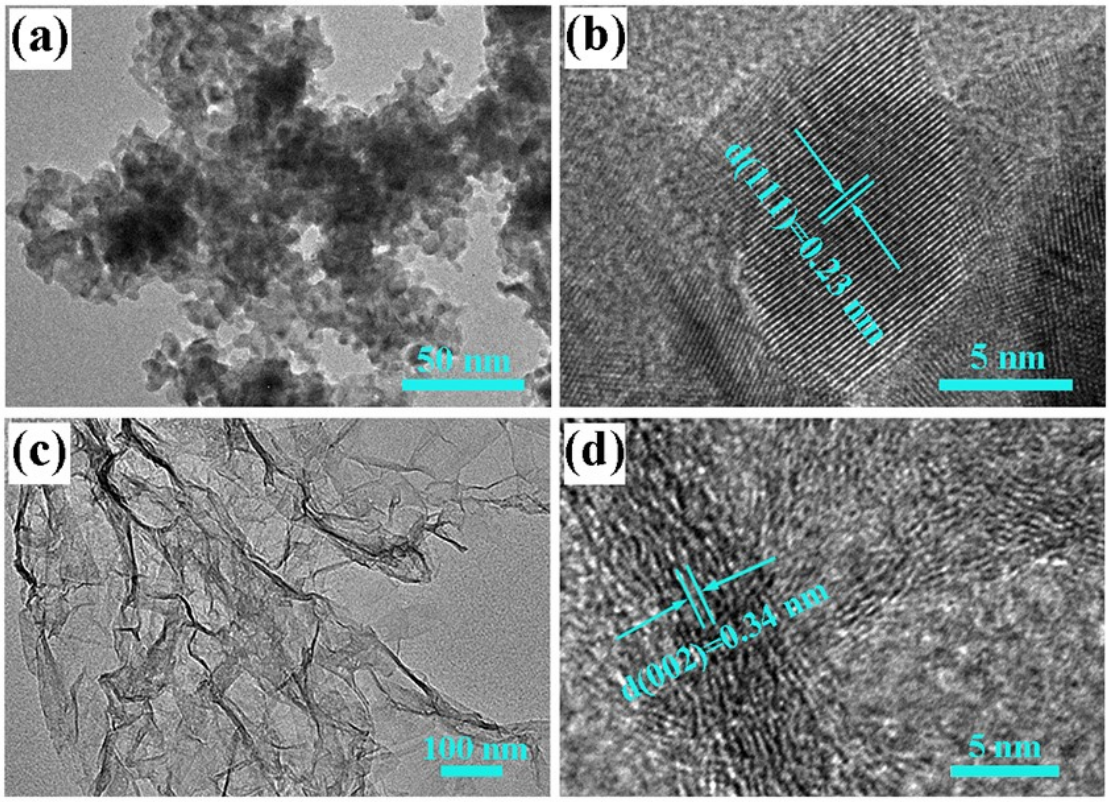

Fig. S4. TEM and HRTEM images of (a) and (b) Pd NPs, (c) and (d) rGO NSs.

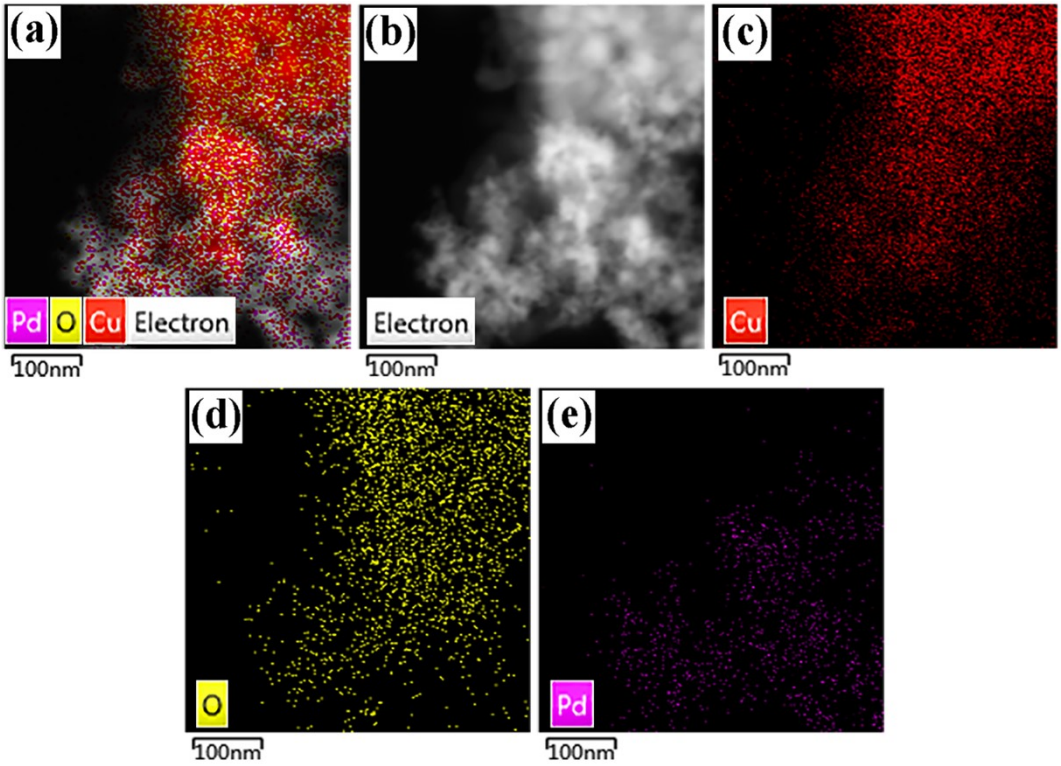

Fig. S5. TEM-EDS element mappings of Pd-CuO and corresponding elemental mapping images.

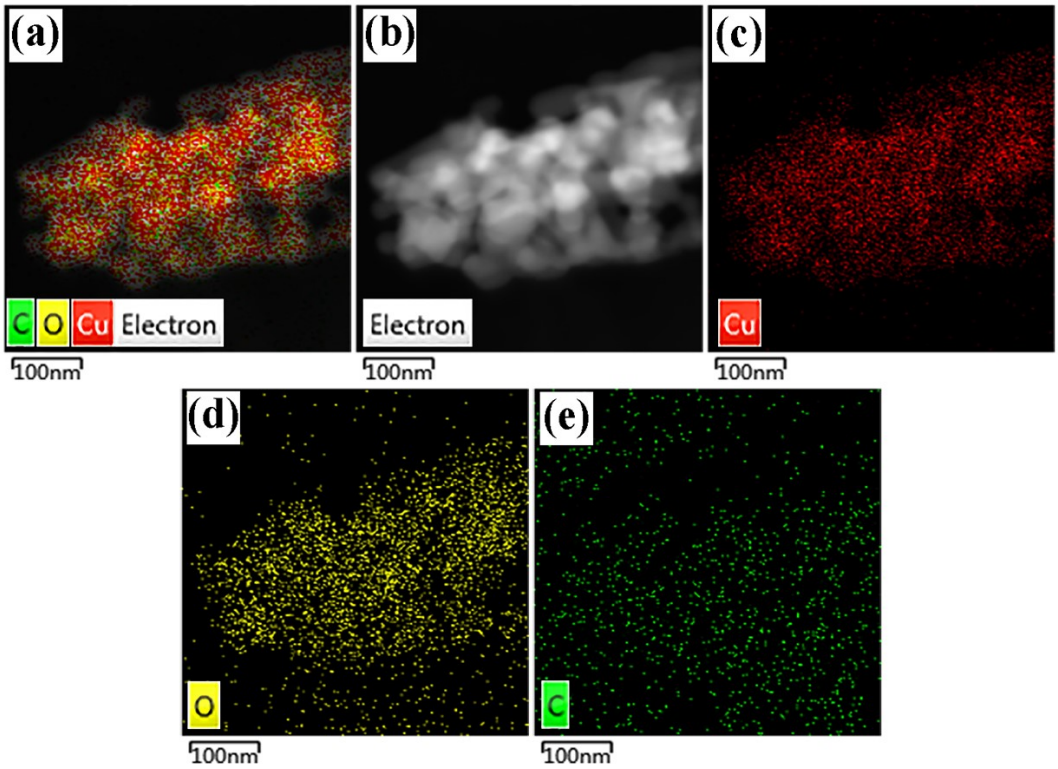

Fig. S6. TEM-EDS element mappings of CuO/rGO and corresponding elemental mapping images.

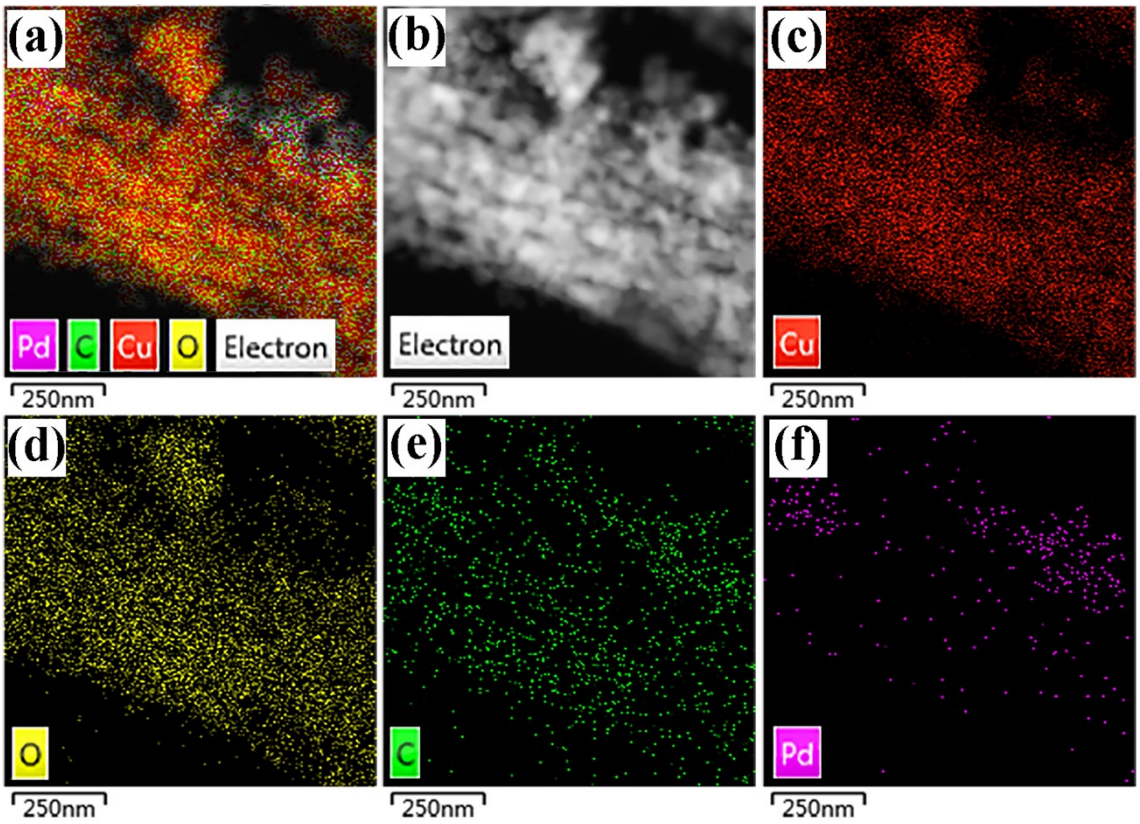

Fig. S7. TEM-EDS element mappings of Pd-CuO/rGO and corresponding elemental mapping images.

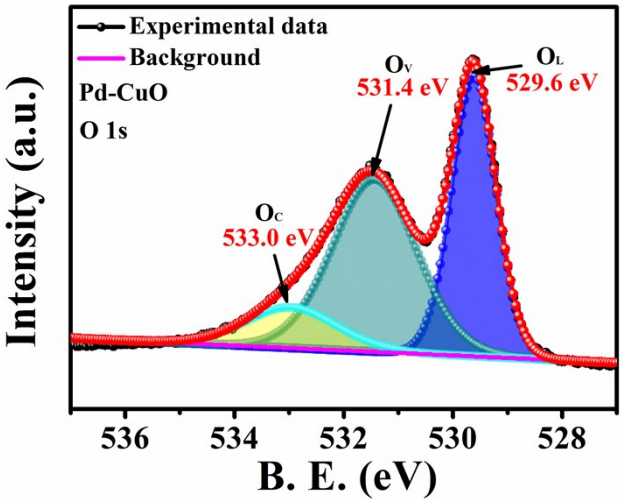

Fig. S8. XPS spectra of O 1s for Pd-CuO.

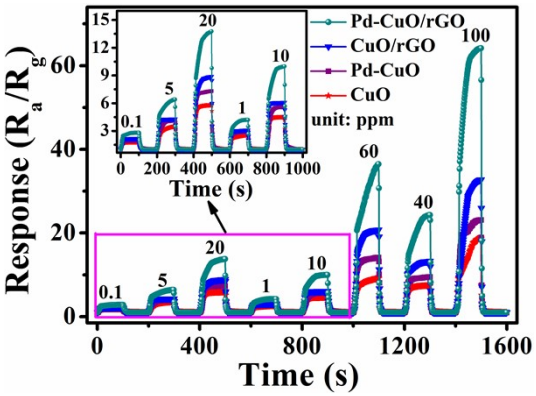

Fig. S9. Response curves of these four sensors as a function of uncontinuously increasing NO_2 gas concentrations at 23℃.

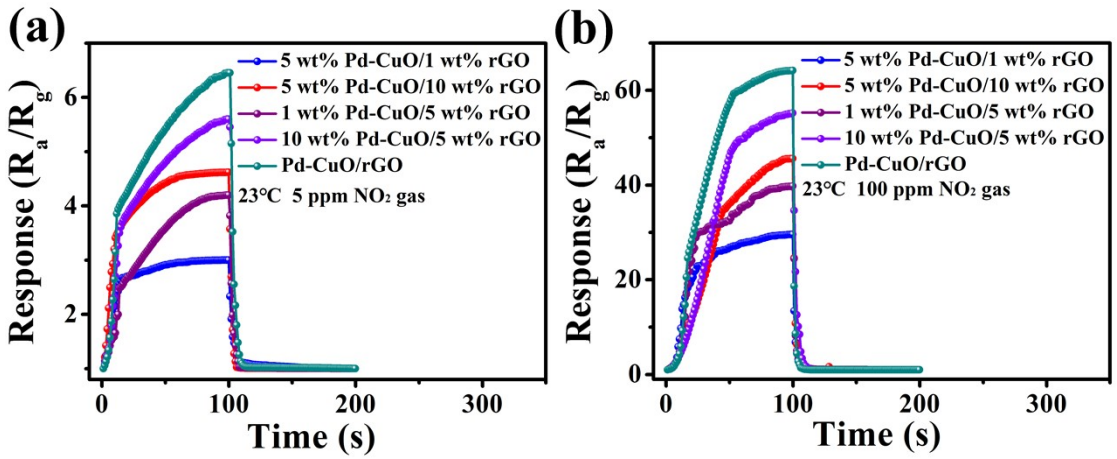

Fig. S10. Response curves of the sensors exposed to 5 and 100 ppm NO_2 gas with different concentrations of Pd and rGO at 23°C.

Table S1. The response values (S) of these four sensors as a function of NO_2 gas concentration at 23°C.

Products	50 ppb	100 ppb	1 ppm	5 ppm	10 ppm	20 ppm	40 ppm	60 ppm	80 ppm	100 ppm
CuO	1.1	1.8	2.5	3.5	4.5	5.8	7.4	9.2	13.1	18.7
Pd-CuO	1.3	1.9	2.9	4.1	5.6	7.5	9.6	14.2	18.7	23.9
CuO/rGO	1.5	2.2	3.1	4.3	6.1	8.9	13.3	20.6	28.7	32.8
Pd-CuO/rGO	1.7	2.8	4.2	6.5	10.1	13.8	24.5	36.5	51.9	64.2

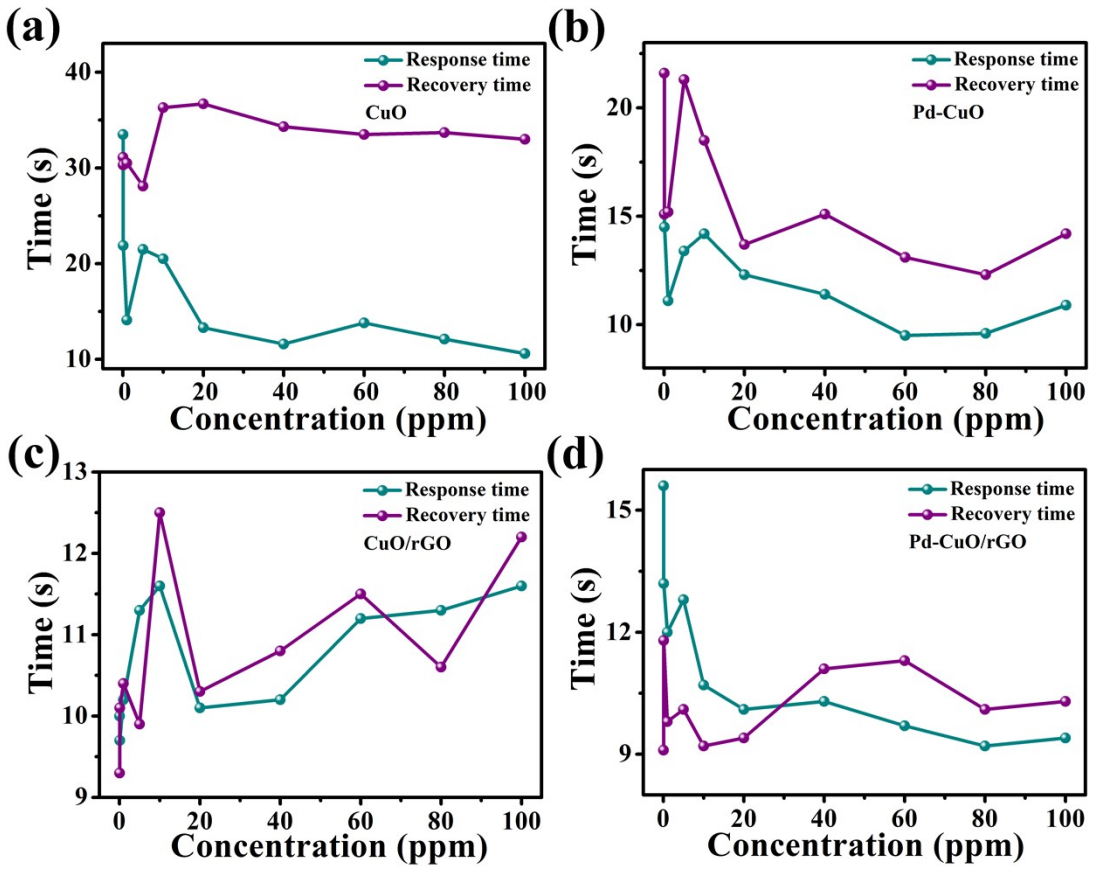

Fig. S11. Response and recovery time of these four sensors towards various concentrations of NO_2 gas ranging from 50 ppb to 100 ppm at 23℃.

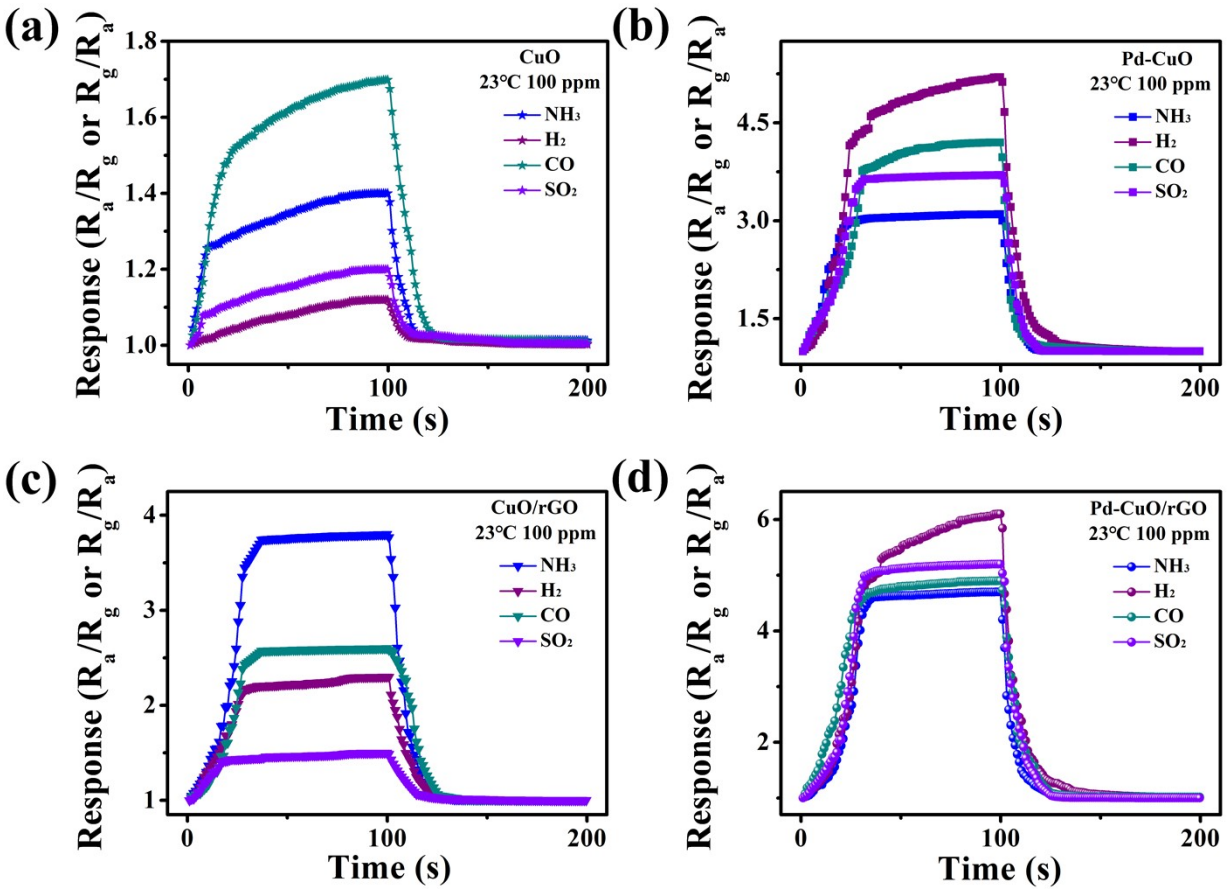

Fig S12. The corresponding response values of these four sensors towards 100 ppm NH_3, H_2, CO and SO_2 gases at 23℃.

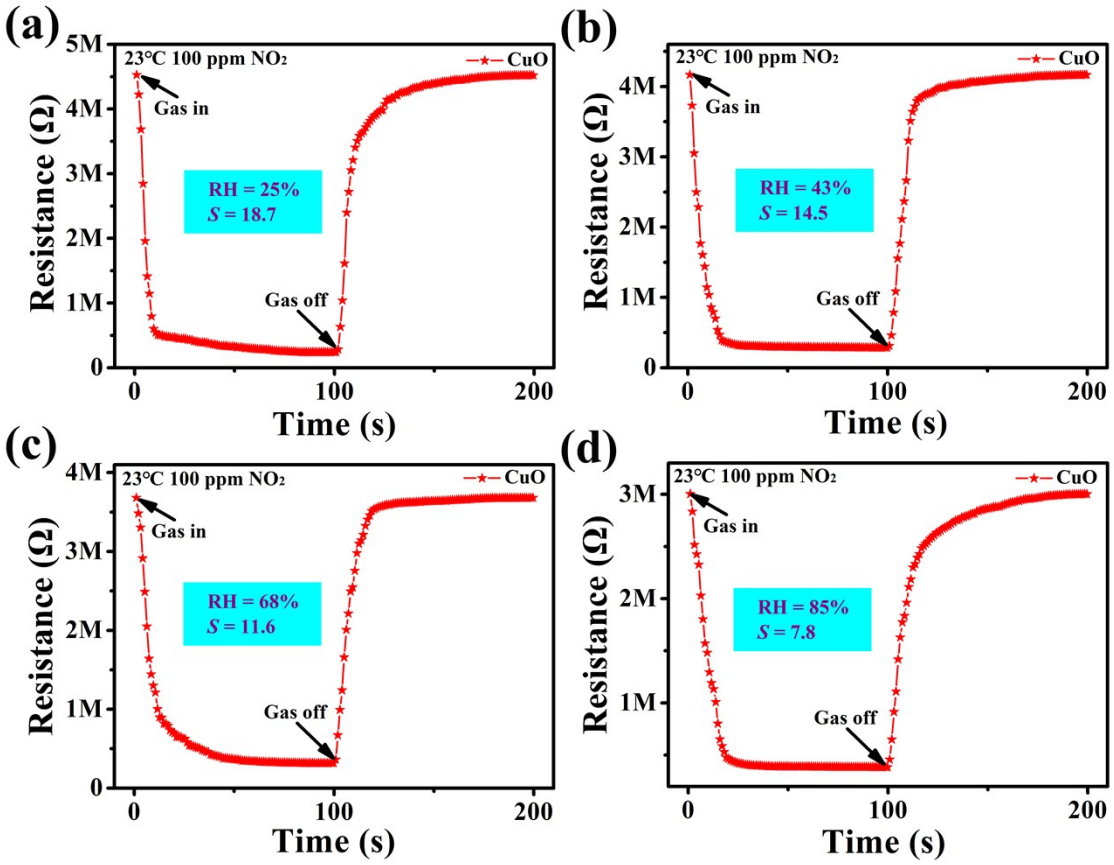

Fig. S13. Dynamic resistance changes of the CuO sensor under different RH conditions towards 100 ppm NO_2 gas at 23°C.

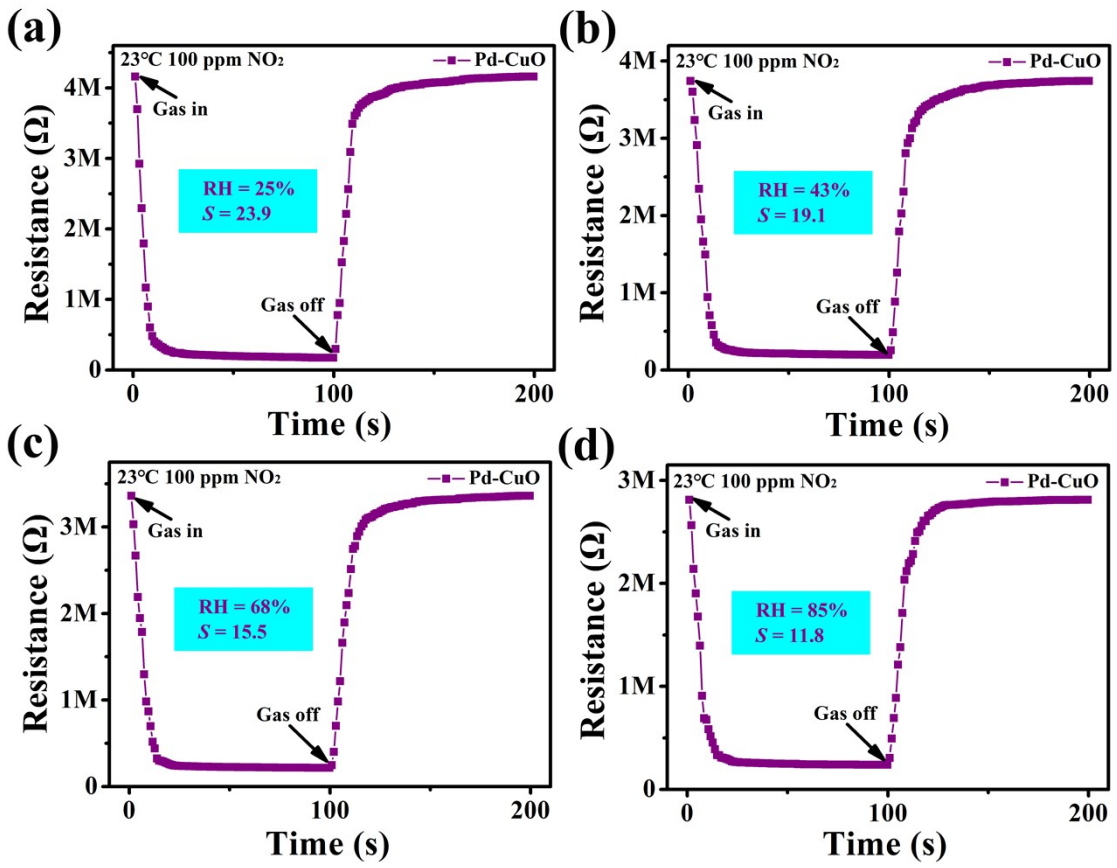

Fig. S14. Dynamic resistance changes of the Pd-CuO sensor under different RH conditions towards 100 ppm NO_2 gas at 23°C.

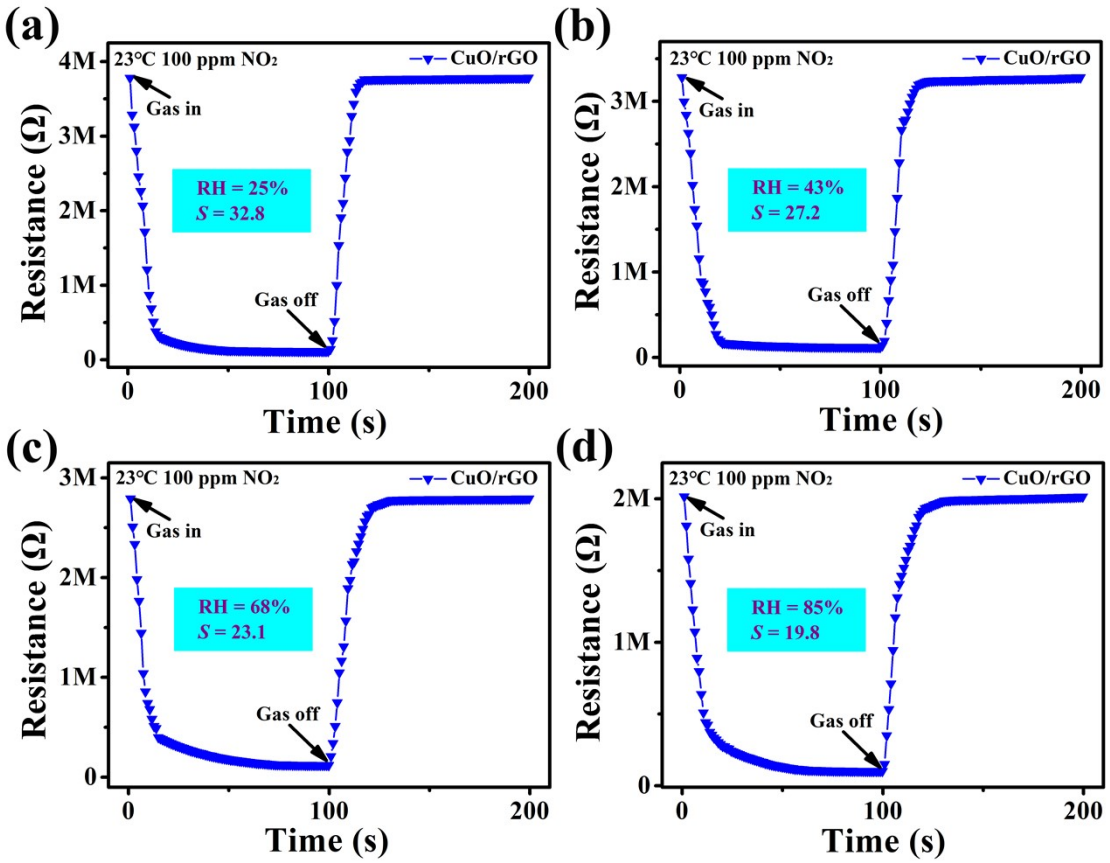

Fig. S15. Dynamic resistance changes of the CuO/rGO sensor under different RH conditions towards 100 ppm NO_2 gas at 23°C.

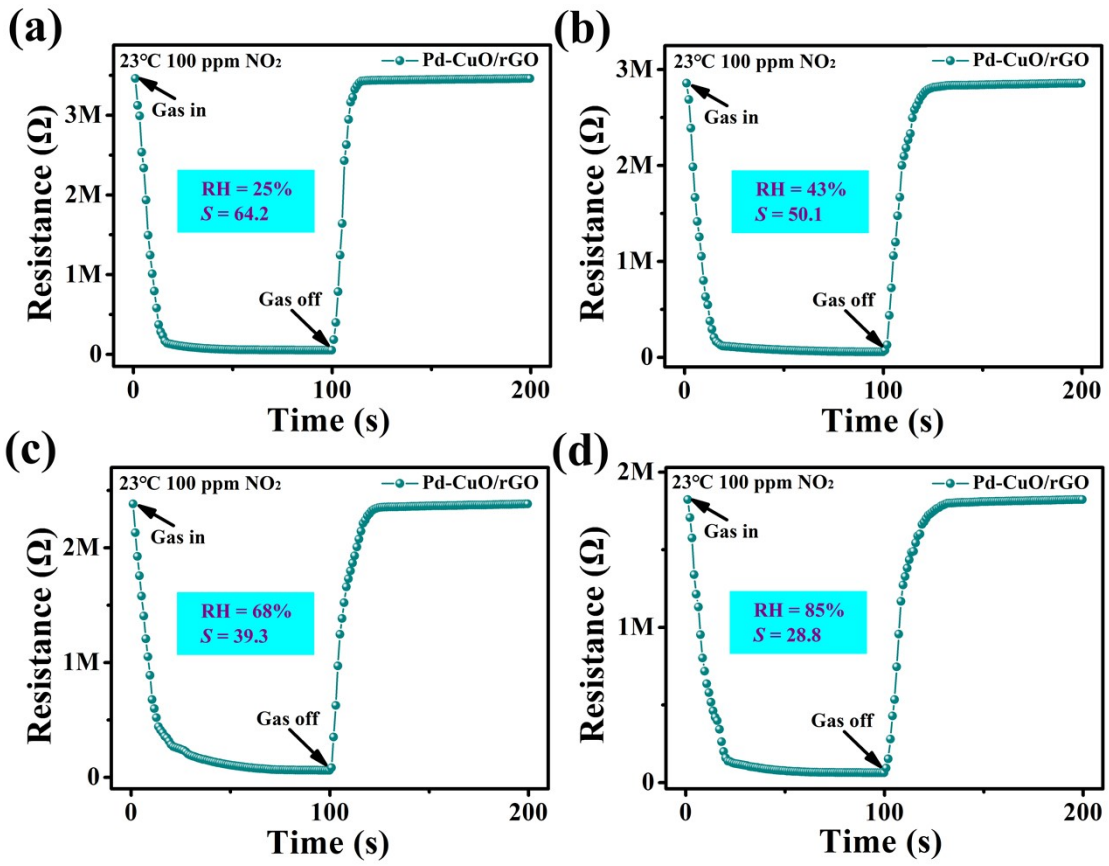

Fig. S16. Dynamic resistance changes of the Pd-CuO/rGO sensor under different RH conditions towards 100 ppm NO_2 gas at 23°C.

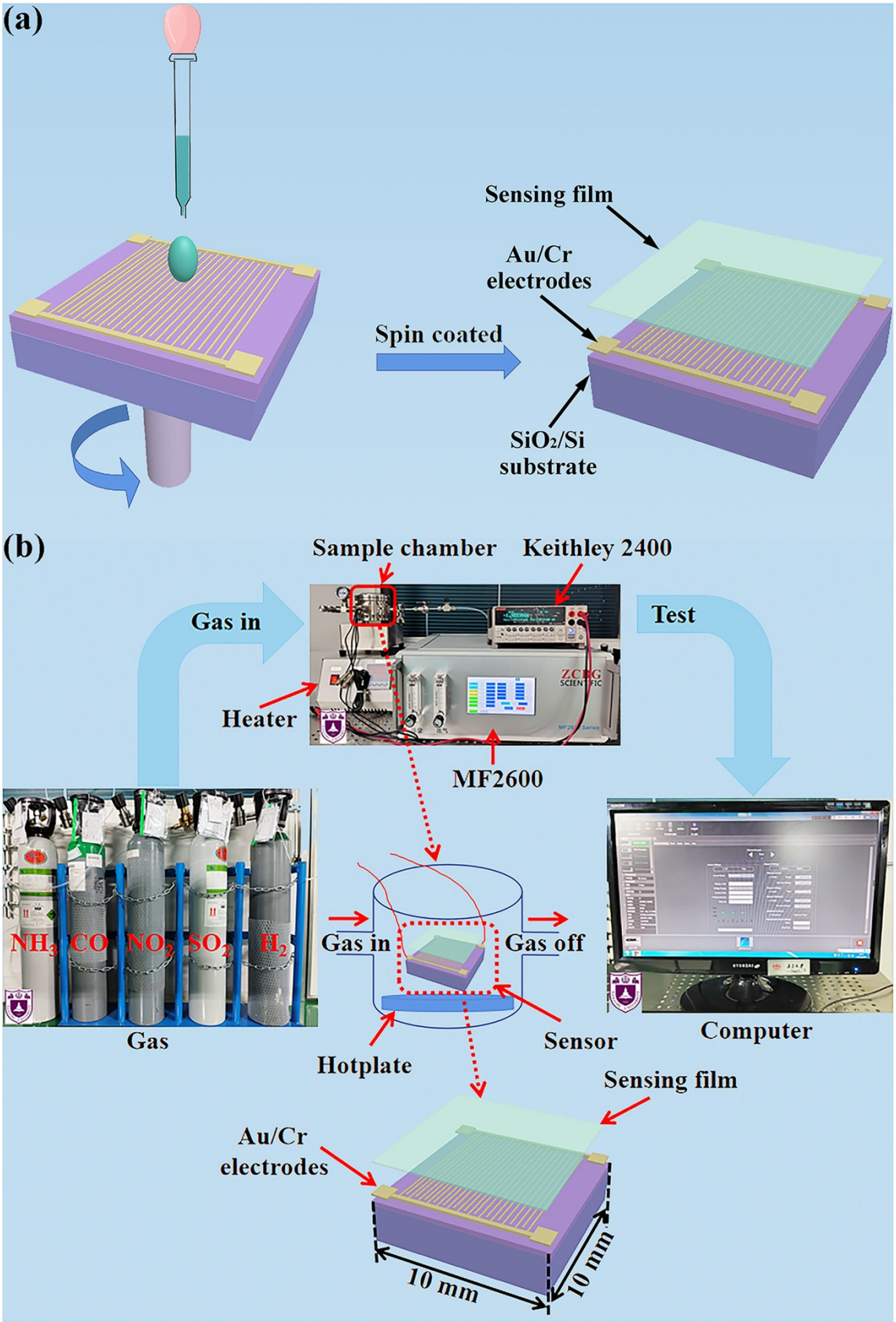

Fig. S17. Schematic diagram of (a) the fabrication process and (b) the test setup for the gas sensor.